

# Finite-time Landau-Zener processes and counter-diabatic driving in open systems: beyond Born, Markov and Rotating-wave approximations

Zhe Sun,<sup>1,2,\*</sup> Longwen Zhou,<sup>2</sup> Gaoyang Xiao,<sup>2</sup> Dario Poletti,<sup>3,4,†</sup> and Jiangbin Gong<sup>2,‡</sup>

<sup>1</sup>*Department of Physics, Hangzhou Normal University, Hangzhou 310036, China*

<sup>2</sup>*Department of Physics, National University of Singapore, Singapore 117542*

<sup>3</sup>*Singapore University of Technology and Design, 8 Somapah Road, 487372 Singapore*

<sup>4</sup>*MajuLab, CNRS-UNS-NUS-NTU International Joint Research Unit, UMI 3654, Singapore*

We investigate Landau-Zener processes modeled by a two-level quantum system, with its finite bias energy varied in time and in the presence of a single broadened cavity mode at zero temperature. By applying the hierarchy equation method to the Landau-Zener problem, we computationally study the survival fidelity of adiabatic states without Born, Markov, rotating-wave or other perturbative approximations. With this treatment it also becomes possible to investigate cases with very strong system-bath coupling. Different from a previous study of infinite-time Landau-Zener processes, the fidelity of the time-evolving state as compared with instantaneous adiabatic states shows non-monotonic dependence on the system-bath coupling and on the sweep rate of the bias. We then consider the effect of applying a counter-diabatic driving field, which is found to be useful in improving the fidelity only for sufficiently short Landau-Zener processes. Numerically exact results show that different counter-diabatic driving fields can have much different robustness against environment effects. Lastly, using a case study we discuss the possibility of introducing a dynamical decoupling field in order to eliminate the decoherence effect of the environment and at the same time to retain the positive role of a counter-diabatic field. Our work indicates that finite-time Landau-Zener processes with counter-diabatic driving offer a fruitful test bed to understand controlled adiabatic processes in open systems.

PACS numbers: 42.50.Dv, 03.65.Yz

## I. INTRODUCTION

Landau-Zener (LZ) transitions happen when the bias energy of a quantum two-level system is swept through an avoided level crossing. For a sweep with a constant rate from time  $t = -\infty$  to  $+\infty$ , the LZ problem is exactly solvable and the final survival probability of the adiabatic state can be obtained asymptotically [1]. LZ transitions have attracted considerable interest both theoretically and experimentally [2–7]. It has been used to model dynamical processes in a variety of physical systems [8, 9]. For instance, with superconducting circuits, which can behave as controllable quantum two-level systems, LZ and Landau-Zener-Stückelberg problems were studied by several groups [10–13]. LZ processes controlled by classical or quantized light fields were also studied in [14–16].

The influence of environment on quantum systems has motivated numerous studies on the dissipative LZ problem. Exact results are available at zero temperature [17, 18], analytical discussions based on perturbation expansions were derived in [19, 20], and various numerical methods were employed for the finite-temperature situations [21–28]. The non-monotonic dependence of the LZ transition probability on the sweep rate was studied in [21] using a numerically exact method. Environment

parameters, such as temperature, can exponentially enhance the coherent oscillations generated at a LZ transition [23]. Transversal system-bath interactions were found to influence the survival probability more strongly than longitudinal system-bath interactions [25, 26].

Put in a more general perspective, the manipulation of instantaneous eigenstates of a quantum system along its adiabatic paths can be very useful. In order to avoid nonadiabatic transitions, the operation has to be executed over a long time scale. Unavoidably, however, a slower process would allow more unwanted decoherence effects induced by an environment. Hence, on the one hand a process should be slow such that the system can stay close to adiabatic states. On the other hand, the process should be fast so that not too much decoherence can set in before an adiabatic process ends. This conflict makes it necessary to have a highly reliable treatment of open quantum systems, which can handle, for example, long-time evolutions and sometimes strong system-bath couplings.

Usually, the description of the dynamics of open systems starts with a perturbative theory and involves various approximations, such as the Born, Markov and rotating-wave approximation (RWA). An efficient method that avoids the above approximations was developed by Tanimura *et al.* [29–33], who established a set of hierarchical equations that includes all orders of system-bath interactions. The hierarchy equation method has been successfully employed to describe the quantum dynamics of various physical, chemical and biophysical systems [32, 34–36]. In addition, the hierarchy equation

---

\*Electronic address: [sunzhe@hznu.edu.cn](mailto:sunzhe@hznu.edu.cn)

†Electronic address: [dario\\_poletti@sutd.edu.sg](mailto:dario_poletti@sutd.edu.sg)

‡Electronic address: [phygj@nus.edu.sg](mailto:phygj@nus.edu.sg)

method can be used to study the dynamics of qubit devices operating at low temperatures [37, 38], when the environment is usually modelled by a Lorentz-broadened cavity mode. For these reasons, we shall use the hierarchy equation method to exactly study LZ processes under the influence of an environment. In particular, we focus on finite-time LZ processes coupled to an environment. We shall also vary the system-bath coupling strength from weak to arbitrarily strong regimes, observing a non-monotonic dependence of the survival fidelity on the coupling strength. This result indicates that a finite-time LZ process can behave much differently from the more idealized LZ process that starts and ends with an infinite energy bias [17].

To shorten the time scale of a useful quantum adiabatic operation, various protocols have been proposed to suppress the nonadiabatic transitions with additional control fields. Such protocols are often called counterdiabatic (CD) driving, shortcuts to adiabaticity, or transitionless driving [39–47]. Following Ref. [40–42], we refer to all such quantum control strategies as CD drivings. Some of them have been implemented in harmonic systems [48], atom transport [49], quantum computing [50], quantum simulations [51], many-body state engineering [52], cooling of nanomechanical resonators [53], and so on. CD drivings have also been suggested as a way to improve the performance of quantum heat engines [54], although with due attention to the cost of using them [55]. Recently, CD driving was also considered in open systems [56, 57]. However, these studies were based on a simplified treatment of the environment.

In this work we investigate the effectiveness of different CD driving protocols in boosting the fidelity values of LZ processes in the presence of an environment. Our investigation is the first of this kind without making any approximations. From our numerically exact results, it is found that not all CD driving fields can perform well in the presence of decoherence. While in the fast driving limit (the associated CD driving field will have extremely large peak values) all CD driving fields can expectedly do a good job, in the cases with intermediate sweep rates, the addition of a CD driving field may even degrade the fidelity. The specific implementation of a CD driving field may also have a large impact on the fidelity. These results clearly show that if the total time scale of an adiabatic process cannot be made very short (e.g., due to hardware implementations or the bandwidth limit of the CD driving), then the introduction of an additional control field, whose aim is mainly to suppress the system-environment coupling, can still be of interest. In the literature a control field capable of modulating and hence suppressing the system-bath coupling is often called a dynamical decoupling (DD) field [58, 59]. Using a case study at the end of this work, we indeed discuss the possibility of combining a CD driving field with a DD field together.

This paper is organized as follows: in Sec. II we introduce the model system and the hierarchy equation method. In Sec. III we show the numerical results of

our finite-time LZ dynamics under the influence of an environment. In Sec. IV, two types of CD drivings are considered and compared. In Sec. V, we discuss and numerically study a possible combination of CD driving and a continuous DD field. Finally, Sec. VI concludes this paper.

## II. SYSTEM-ENVIRONMENT MODEL AND HIERARCHY EQUATION METHOD

### A. Models, parameters and initial conditions

We consider a driven two-level system interacting with a bosonic bath. The total Hamiltonian is ( $\hbar = 1$  is assumed throughout)

$$H_{\text{tot}} = H_S(t) + H_B + H_{\text{SB}}, \quad (1)$$

where the system-Hamiltonian is chosen to be of LZ-type, i.e.,  $H_S = H_{\text{LZ}}$ , with

$$H_{\text{LZ}} = Z(t) \frac{\sigma_z}{2} + X \frac{\sigma_x}{2}, \quad (2)$$

where  $\sigma_{x,y,z}$  are Pauli matrices. A positive and time-independent constant  $X$  is employed to characterize the interaction between the two diabatic states  $|\uparrow\rangle$  and  $|\downarrow\rangle$  (the eigenstates of  $\sigma_z$ ). We assume the following time-dependent parameter

$$Z(t) = \frac{(z_f - z_0)}{t_f} t + z_0, \quad (3)$$

which describes a linearly varying bias-energy between the diabatic states, with  $Z(t) \in [z_0, z_f]$  (let  $z_0 = -z_f$  and  $z_0 < 0$  in this paper) and  $t \in [0, t_f]$ . The duration of a LZ process is hence  $t_f$  and the sweeping rate becomes  $v = (z_f - z_0)/t_f$ . In our study, the boundary of the bias-energy, determined by  $z_0$  and  $z_f$ , is independent of  $t_f$ . By tuning  $t_f$ , we can study the cases of different sweeping rates. Here, one should note the difference between the form of Eq. (3) and the conventional LZ driving, i.e.,  $Z(t) = vt$ . In the latter, changing the evolution time interval is equivalent to changing the boundary of the bias-energy. Note also that in pure theoretical considerations, an infinite time interval, i.e.,  $t \in (-\infty, \infty)$  is often chosen because it allows greater analytical insight, however this implies an infinite energy bias and is not adopted here.

Now let us briefly recall several results about the standard LZ problem described by the Hamiltonian in Eq. (2). For  $X = 0$  the diabatic states  $|\uparrow\rangle$  and  $|\downarrow\rangle$  with bias-energies  $\pm Z(t)/2$  cross at  $t = t_f/2$  linearly. When  $X \neq 0$ , the diabatic states are not eigenstates of the Hamiltonian in Eq. (2), and an avoided-level crossing appears between the adiabatic energy-levels  $E_{\pm}(t) = \pm \sqrt{[Z(t)]^2 + X^2}/2$  at  $t = t_f/2$ . Thus, in general, some population transfer occurs. If the bias energy  $Z(t)$  is swept from a large negative value to a large positive value, the diabatic states

coincide with the initial and final adiabatic states. Then it is possible to compute the survival probability of the qubit ending up in the initial adiabatic state of  $H_{LZ}$ , which is  $P_{LZ} = 1 - \exp[-\pi X^2/(2v)]$ . In the adiabatic limit  $X^2/v \gg 1$ ,  $P_{LZ}$  will saturate at 1.

To consider a LZ process in the presence of an environment, we model a bosonic environment by the bath Hamiltonian  $H_B$  and the system-bath coupling by Hamiltonian  $H_{SB}$ ,

$$H_B = \sum_k \omega_k b_k^\dagger b_k, \quad (4)$$

$$H_{SB} = V \sum_k \left( g_k b_k + g_k^* b_k^\dagger \right), \quad (5)$$

where  $\omega_k$  indicates the frequency of the  $k$ -th mode of the bath.  $b_k^\dagger$  and  $b_k$  are the creation and annihilation operators of the bath.  $V = g_z \sigma_z + g_x \sigma_x$  denotes the system operators and it includes longitudinal ( $\sigma_z$ ) and transversal ( $\sigma_x$ ) couplings with the mixing coefficient  $g_z$  and  $g_x$ , respectively.  $g_k$  denotes the individual coupling strength between the qubit and the  $k$ -th mode of the bath. In the following sections, we focus on the transversal coupling by setting  $g_z = 0$ ,  $g_x = 1/2$ . This is because transversal interactions in general have stronger influence on population transitions than longitudinal interactions at the same coupling strength [17, 25, 26].

The environment is chosen to simulate a single mode of a leaking cavity. Due to the imperfection of the cavity, the single mode is broadened into a continuous distribution with a center frequency  $\omega_c$ , and the qubit-cavity coupling spectrum is usually of a Lorentz-type [37, 60], i.e.,

$$J(\omega) = \frac{1}{\pi} \frac{\gamma \lambda}{(\omega - \omega_c)^2 + \lambda^2}, \quad (6)$$

where  $\lambda$  characterizes the broadening width of the cavity mode (i.e., damping rate), which is connected to the bath correlation time  $\tau_B \sim \lambda^{-1}$ . The perfect-cavity limit is obtained for  $\lambda \rightarrow 0$ , which results in  $J(\omega) = \gamma \delta(\omega - \omega_c)$ . The parameter  $\gamma$  reflects the overall system-bath coupling strength.

The total system is assumed to start from a product state, i.e.,

$$\rho_{\text{tot}}(0) = \rho_S(0) \otimes \rho_B(0), \quad (7)$$

where the initial state of the system can be chosen as the ground state of  $H_{LZ}$  in Eq. (2) at  $t = 0$ . That is, the initial system density matrix is given by

$$\rho_S(0) = |\psi_g(0)\rangle \langle \psi_g(0)|, \quad (8)$$

where  $|\psi_g(t)\rangle = -\sin \frac{\theta_t}{2} |\uparrow\rangle + \cos \frac{\theta_t}{2} |\downarrow\rangle$  is the adiabatic ground state with the time-dependent superposition coefficient  $\theta_t = \arccot[Z(t)/X]$ . Let  $t = 0$ , one will obtain the initial ground state corresponding to  $\theta_0 = \arccot[z_0/X]$ . The adiabatic excited state is

$|\psi_e(t)\rangle = \cos \frac{\theta_t}{2} |\uparrow\rangle + \sin \frac{\theta_t}{2} |\downarrow\rangle$ . The cavity mode is assumed to be at zero temperature and starts from a vacuum state  $|\psi_B(0)\rangle = \otimes_k |0\rangle_k$ . The initial bath density matrix is hence given by  $\rho_B(0) = |\psi_B(0)\rangle \langle \psi_B(0)|$ .

## B. Hierarchy equation method

For the product form of the initial system-bath state  $\rho_{\text{tot}}(0) = \rho_S(0) \otimes \rho_B(0)$ , the exact dynamics of the system in the interaction picture can be derived as [29, 31]

$$\rho_S^{(I)}(t) = \hat{\mathcal{T}} \exp \left\{ - \int_0^t dt_2 \int_0^{t_2} dt_1 V^\times(t_2) [C^R(t_2 - t_1) V^\times(t_1) + iC^I(t_2 - t_1) V^\circ(t_1)] \right\} \rho_S(0), \quad (9)$$

where  $\hat{\mathcal{T}}$  is the chronological time-ordering operator, which orders the operators inside the integral such that the time arguments increase from right to left. Two superoperators are introduced,  $A^\times B \equiv [A, B] = AB - BA$  and  $A^\circ B \equiv \{A, B\} = AB + BA$ , which simplifies the dynamical equation as well as the following derivation of the hierarchy equations. In above  $C^R(t_2 - t_1)$  and  $C^I(t_2 - t_1)$  are the real and imaginary parts of the bath time-correlation function

$$\begin{aligned} C(t_2 - t_1) &\equiv \text{Tr} [B(t_2) B(t_1) \rho_B(0)] \\ &= \gamma \exp[-(\lambda + i\omega_c) |t_2 - t_1|], \end{aligned} \quad (10)$$

respectively, and

$$B(t) = \sum_k \left( g_k b_k e^{-i\omega_k t} + g_k^* b_k^\dagger e^{i\omega_k t} \right). \quad (11)$$

Note that in Eq. (10) the bath correlation is already assumed to be an exponential form, a form required to derive the hierarchy equations. In the single-mode limit  $\lambda \rightarrow 0$ , we have  $C(t_2 - t_1) \rightarrow \gamma \exp(-i\omega_c |t_2 - t_1|)$ .

To present the hierarchy equations (for completeness) in a convenient form, we further write the real and imaginary parts of the time-correlation function (10) as

$$C^R(t) = \sum_{k=1}^2 \frac{\gamma}{2} e^{-\nu_k t}, \quad C^I(t) = \sum_{k=1}^2 (-1)^k \frac{\gamma}{2i} e^{-\nu_k t}, \quad (12)$$

where  $\nu_k = \lambda + (-1)^k i\omega_0$ . Then, following the procedures shown in [29, 31], the hierarchy equations of the qubit are found to be

$$\begin{aligned} \frac{\partial}{\partial t} \varrho_{\vec{n}}(t) &= - (iH_S^\times + \vec{n} \cdot \vec{\nu}) \varrho_{\vec{n}}(t) - i \sum_{k=1}^2 V^\times \varrho_{\vec{n} + \vec{e}_k}(t) \\ &\quad - i \frac{\gamma}{2} \sum_{k=1}^2 n_k \left[ V^\times + (-1)^k V^\circ \right] \varrho_{\vec{n} - \vec{e}_k}(t), \end{aligned} \quad (13)$$

where the subscript  $\vec{n} = (n_1, n_2)$  is a two-dimensional index, with integer numbers  $n_{1(2)} \geq 0$ , and  $\rho_S(t) \equiv$

$\varrho_{(0,0)}(t)$ . The vectors  $\vec{e}_1 = (1, 0)$ ,  $\vec{e}_2 = (0, 1)$ , and  $\vec{\nu} = (\nu_1, \nu_2) = (\lambda - i\omega_c, \lambda + i\omega_c)$ . We emphasize that  $\varrho_{\vec{n}}(t)$  with  $\vec{n} \neq (0, 0)$  are auxiliary operators introduced only for the sake of computing, they are not density matrices, and are all set to be zero initially. The hierarchy equations are a set of linear differential equations, and can thus be solved using, for example, the Runge-Kutta method. The contributions of the bath to the dynamics of the system, including both dissipation and Lamb shift, are fully contained in the hierarchy equation (13).

For numerical computations, the hierarchy equations (13) must be truncated for a large enough  $\vec{n}$ . We can increase the hierarchy order  $\vec{n}$  until the results of  $\rho_S(t)$  converge. The terminator of the hierarchy equation is

$$\begin{aligned} \frac{\partial}{\partial t} \varrho_{\vec{N}}(t) = & - \left( iH_S^X + \vec{N} \cdot \vec{\nu} \right) \varrho_{\vec{N}}(t) \\ & - i\frac{\gamma}{2} \sum_{k=1}^2 n_k \left[ V^\times + (-1)^k V^\circ \right] \varrho_{\vec{N}-\vec{e}_k}(t), \end{aligned} \quad (14)$$

where we dropped the deeper auxiliary operators  $\varrho_{\vec{N}+\vec{e}_k}$ . The numerical results in this paper were all converged, and the density matrix  $\rho_S(t)$  was tested to be positive. The detailed derivation of Eq.(13) can be found in Refs. [29, 37].

### III. FINITE-TIME LANDAU-ZENER PROCESSES IN AN ENVIRONMENT

We are now ready to investigate, using numerically exact results, the features of finite-time LZ processes in an environment modeled above. Some parameters are fixed throughout, i.e., for an arbitrary energy unit, we choose the scaled values  $X = 0.5$ ,  $z_f = -z_0 = 6$ ,  $\lambda = 0.5$  and  $\omega_c = 0.5$ , where a relatively large initial and final bias-energy is chosen, i.e.,  $|z_0| = |z_f| = 12X$ , and the central frequency of the bath is assumed to be equal to the minimal energy gap of the adiabatic states, i.e.,  $\omega_c = X$ .

In conventional physical systems, the intrinsic energy scale of the system is larger than the energy-scale of the system-bath coupling. However, in artificial quantum devices [10, 11], this may not be the case. Therefore, we consider both weak and strong coupling cases and this is possible because the hierarchy equation method is not perturbative.

One central quantity in our investigation is  $F(t) = |\langle \psi_g(t) | \rho(t) | \psi_g(t) \rangle|$ , which describes the overlap between the actual time-evolving state and the target instantaneous ground state. In Fig.1(a), we show  $F(t)$  versus the scaled time  $t/t_f$  for different values of  $\gamma$ . The (red) solid line displays the case without environment ( $\gamma = 0$ ), wherein a high final fidelity is found. This high fidelity can be attributed to the slow sweeping rate of  $v = 0.12$  ( $t_f = 100$ ), which gives a large ratio of  $X^2/v \approx 2.1$ . Indeed, if the final fidelity approximately obeys the standard LZ probability formula

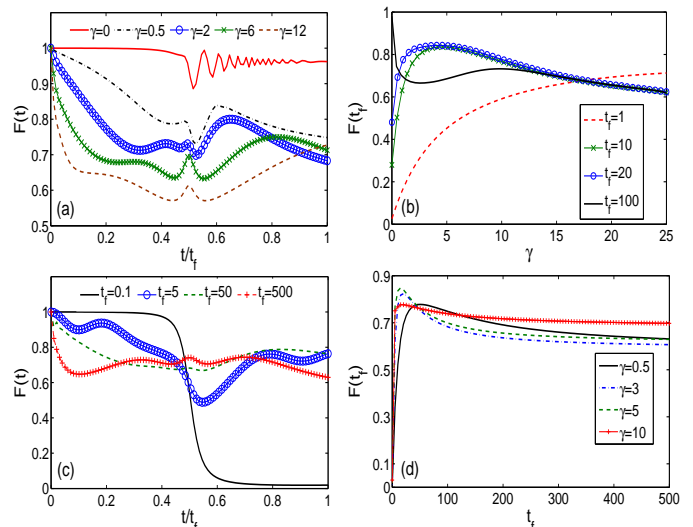


Figure 1: (Color online) (a) The fidelity with instantaneous adiabatic states, defined as  $F(t) = \langle \psi_g(t) | \rho(t) | \psi_g(t) \rangle$ , versus scaled time  $t/t_f$  for different values of the system-bath coupling strength parameter  $\gamma$ . The duration of the finite-time LZ processes is chosen to be  $t_f = 100$ . (b) Final fidelity, defined as  $F(t_f) = \langle \psi_g(t_f) | \rho(t_f) | \psi_g(t_f) \rangle$ , versus  $\gamma$  for different durations of the LZ processes. (c) The fidelity with instantaneous adiabatic states versus scaled time  $t/t_f$  for different values of  $t_f$ , with  $\gamma = 5$ . (d) Final fidelity versus  $t_f$  for different values of  $\gamma$ . Other system and environment parameters are given by  $z_f = -z_0 = 6$ ,  $X = 0.5$  [see Eq. (2)] and  $\omega_c = 0.5$  [see Eq. (6)]. As explained in the main text, all plotted quantities in this work are dimensionless.

$F(t_f) \approx 1 - \exp[-\pi X^2/(2v)]$  [note, strictly speaking, this formula is only for an infinite-time LZ with  $t \in (-\infty, \infty)$ ], one expects the final fidelity close to unity. However for  $\gamma \neq 0$  the fidelity is strongly affected. Before the LZ transition point at  $t/t_f = 1/2$ , an increase in the system-bath coupling strength  $\gamma$  leads to a decrease in the fidelity. After the LZ transition point, a larger  $\gamma$  can result in increased fidelity, i.e., there exists a non-monotonic dependence of the final fidelity on the coupling strength  $\gamma$ .

This interesting nonmonotonic behavior is shown even more clearly in Fig.1(b), where we plot the final fidelity  $F(t_f)$  versus  $\gamma$  for different durations of a LZ process. The (black) solid line describes a case with a slow sweep rate of  $v = 0.12$  ( $t_f = 100$ ), wherein the LZ time scale [1], i.e.,  $\tau_{LZ} \sim \max[X/v, 1/\sqrt{v}]$  is larger than the bath correlation time  $\tau_B \sim 1/\lambda$ . For this case there is enough time for the environment to influence the LZ process. With the increase of  $\gamma$ , we find first a local minimum of the final fidelity  $F(t_f)$ , then a peak, and finally a gradual decrease. Next we consider shorter processes with  $t_f = 20$  and  $10$ , i.e.,  $v = 0.6$  and  $1.2$ , respectively. The associated time scale  $\tau_{LZ}$  becomes smaller than  $\tau_B$ . In these two cases, the fidelity starts from low values due to the small ratios of  $X^2/v \approx 0.42$  and  $0.21$ . Now, as  $\gamma$  increases, there only exists a peak in the final fidelity. Fur-



ther decreasing the duration to  $t_f = 1$  (i.e.,  $v = 12$ ), the non-monotonic behavior vanishes, so  $F(t_f)$  rises monotonically for the entire shown regime of  $\gamma$ .

Recalling one of the results of Wubs *et al.* [17]

$$F(\infty) = 1 - e^{-\pi W^2/(2v)}, \quad (15)$$

where  $W^2 = X^2 + \gamma$ , and  $\gamma = \int d\omega J(\omega)$  is the effective coupling strength obtained by integrating the spectral density of the environment. In Ref. [17] only a monotonic increase of  $F(t_f)$  versus system-bath coupling was found regardless of whether the sweeping rate is fast or slow. A simple check reveals the origin of the difference. In Ref. [17] a fundamental requirement was that the process was conducted for an infinite evolution time, i.e.,  $t \in (-\infty, \infty)$ . This implies that the initial and final energy bias of the qubit system must be infinitely large as compared with an arbitrarily strong system-bath coupling. In contrast, our finite-time LZ process involves situations for which the system-bath couplings are comparable to the energy bias at the start or in the end. For this reason, a complicated interplay between non-adiabatic transitions and environment-induced excitation or de-excitation can be expected. To confirm this insight, we note that for the studied range of the system parameters, the nonmonotonic behavior discussed above emerges only when the sweeping rate yields a time scale that is comparable with that associated with environment induced transitions.

Similar nonmonotonic phenomena have been found even in an example with pure dephasing dynamics [19, 20]. There the authors analytically obtained the final fidelity based on the first-order adiabatic perturbation theory regarding the sweeping rate  $v$ . The approximate result successfully predicts a minimum of  $F(t_f)$ , which qualitatively agrees with our result shown in Fig. 1(b) for a quite slow sweeping with  $t_f = 100$ . However, it fails to present the maximum of  $F(t_f)$  shown in Fig. 1(b) for stronger system-bath coupling strength, a situation that is definitely beyond a pure-dephasing model.

Fig. 1(c) shows the fidelity versus scaled time for varying durations of LZ processes. The (black) solid line describes the case of fast sweeping ( $t_f = 0.1$ ), where one finds the final fidelity ending at a very small value. For the sake of comparison, we increase  $t_f$  to 5, 50, and 500. As a result, more complex oscillations of  $F(t)$  are observed and the fidelity values after the transition point  $t/t_f = 1/2$  are higher than the fast sweeping case with  $t_f = 0.1$ . Interestingly, the computational results show an upper limit of the final fidelity as  $t_f$  increases. Indeed, the final fidelity for  $t_f = 500$ , is not much different from that with  $t_f = 50$ . This is an obvious environment-induced suppression, which can be seen more clearly in the panel (d), to be discussed next.

In Fig. 1(d), we plot the final fidelity  $F(t_f)$  versus  $t_f$  for different values of the system-bath coupling strength parameter  $\gamma$ . There one can clearly observe the non-monotonic dependence of fidelity on  $t_f$ . For short LZ processes, the final fidelity values are small and different

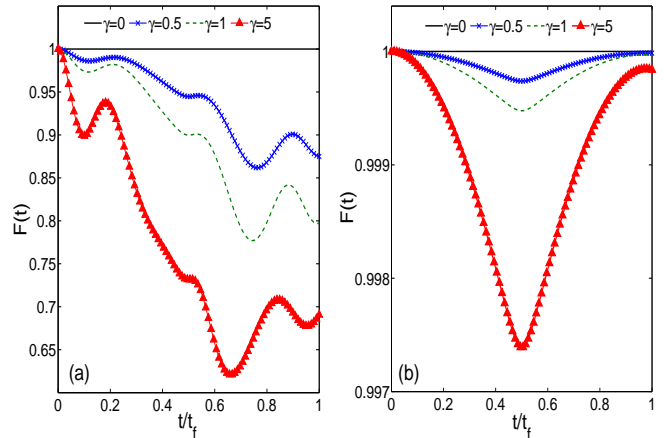


Figure 2: (Color online) The fidelity with instantaneous adiabatic states versus scaled time  $t/t_f$ , for different system-bath coupling strength in the presence of CD driving. The duration of the LZ processes is chosen  $t_f = 5$  in panel (a) and  $t_f = 0.1$  in panel (b). In both panels, the top solid (black) lines correspond to the cases without a bath, i.e.,  $\gamma = 0$ , for which the CD driving leads to perfect unity fidelity. Other system and environment parameters are the same as in Fig. 1. Note that panel (a) and (b) used different scales on the y axis.

system-bath couplings can hardly induce significant differences. With increased  $t_f$ , different values of  $\gamma$  yield different peaks as well as different saturated values of fidelity, constituting interesting features again that are absent in infinite-time LZ processes at zero temperature.

#### IV. LZ PROCESSES WITH COUNTER-DIABATIC DRIVING AND AN ENVIRONMENT

In this section we aim to study how CD driving might improve the fidelity of the time-evolving state in an LZ process (as compared with the instantaneous adiabatic states). We first briefly outline the idea behind the CD driving strategy and then present our results.

##### A. Counter-diabatic driving

A CD [40, 43] driving field is designed to eliminate all unwanted nonadiabatic transitions. Specifically, here the reference Hamiltonian is  $H_{LZ}$  that determines the instantaneous adiabatic states and hence an ideal adiabatic path. One can now construct an auxiliary driving Hamiltonian  $H_{CD}$  to ensure the following: when the system's initial state is prepared in the eigenstate of  $H_{LZ}$  at  $Z = Z(0)$ , i.e.,  $|\psi_n(Z(0))\rangle$ , its ensuing time evolution will track the instantaneous eigenstate  $|\psi_n(Z(t))\rangle$ . To achieve this the following target unitary operation is

required, i.e.,

$$U_{\text{target}} = \sum_n e^{i\phi_n(t)} |\psi_n(Z(t))\rangle \langle \psi_n(Z(0))|, \quad (16)$$

where  $\phi_n$  is a phase factor whose time dependence can be arbitrarily chosen. This unitary evolution can be directly realized by the driving Hamiltonian  $H_S = i\dot{U}_{\text{target}}U_{\text{target}}^\dagger$ , i.e.,

$$H_S = - \sum_n \dot{\phi}_n |\psi_n(Z(t))\rangle \langle \psi_n(Z(t))| + i \sum_n [\partial_t |\psi_n(Z(t))\rangle] \langle \psi_n(Z(t))|. \quad (17)$$

The first term in the above equation is in diagonal form, and so it always commutes with  $H_{\text{LZ}}$ . Due to the freedom in the choice of the phase  $\phi_n(t)$  in Eq. (17), this first term may take many different forms. A typical choice is to make  $\phi_n$  identical with the dynamical phase associated with the ideal adiabatic process naturally generated by  $H_{\text{LZ}}$ . That is,  $\phi_n = -\int_0^t E_n[Z(\tau)]d\tau$ , where  $E_n[Z(t)]$  is the instantaneous eigenvalue of the adiabatic state  $|\psi_n(Z(t))\rangle$ . Under this choice the first term in Eq. (17) is nothing but  $H_{\text{LZ}}$  itself. The second term in the above equation is often called the CD driving field, i.e.,

$$H_{\text{CD}} = i \sum_n [\partial_t |\psi_n(Z(t))\rangle] \langle \psi_n(Z(t))|. \quad (18)$$

Using the specific form of  $|\psi_n(Z(t))\rangle$  for our LZ system, one finds

$$H_{\text{CD}} = \frac{\dot{\theta}_t}{2} \sigma_y, \quad (19)$$

where  $\theta_t = \text{arccot}[Z(t)/X]$ . The system Hamiltonian hence becomes  $H_S = H_{\text{LZ}} + H_{\text{CD}}$ .

From the derivation above, it can be noted that the component  $H_{\text{LZ}}$  in  $H_S$  only provides a dynamical phase during the designed evolution. Different choices of  $\phi_n$  will produce different diagonal operations in the eigenspace spanned by  $|\psi_n(Z(t))\rangle$ . The actual component that is responsible for suppressing non-adiabatic transitions is the  $H_{\text{CD}}$  component. For example, which we will make use of later, if we set  $\phi_n = 0$ , then  $H_S = H_{\text{CD}}$  is equally competent to give rise to an adiabatic evolution path that tracks perfectly the instantaneous adiabatic states  $|\psi_n(Z(t))\rangle$ .

The above design strategy does not have any environment in the picture. The effectiveness of CD driving in the presence of an environment is hence of considerable interest. We now present our computational results on this issue. In Fig. 2, the total system Hamiltonian is chosen as  $H_S = H_{\text{LZ}} + H_{\text{CD}}$ . System and environment parameters such as  $z_0, z_f, X, \omega_c, \lambda$  are the same as those in Fig. 1. We calculate the fidelity versus scaled time  $t/t_f$  for different values of  $\gamma$ . Panel (a) of Fig. 2 shows three cases with  $\gamma$  increasing from 0.5, 1 to 5, all with  $t_f = 5$ , a

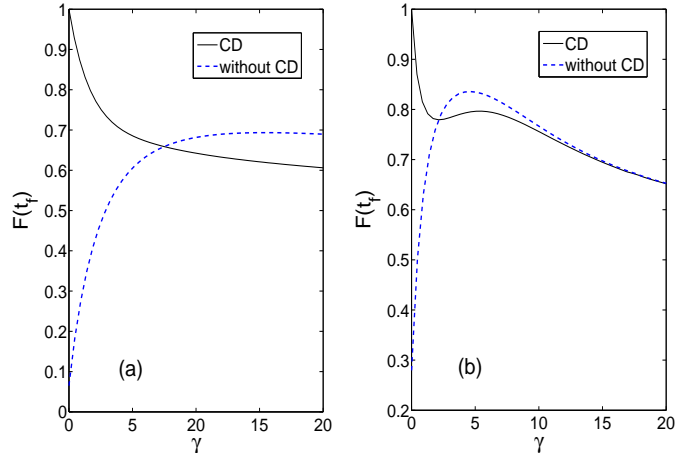


Figure 3: (Color online) The final fidelity values versus the system-bath coupling strength parameter  $\gamma$ , with the total duration of LZ processes given by  $t_f = 2$  in (a) and  $t_f = 10$  in (b), with and without CD driving. Other system and environment parameters are the same as in Fig. 1.

process not too short or too long. It is found that the fidelity  $F(t)$  oscillates with time and becomes much lower than unity in the end. Let us now compare these results with those in Fig. 1(c) also with  $\gamma = 5$  and  $t_f = 5$ , that is, compare the (blue) solid line (connected with circles) in Fig. 1(c) and the (red) solid line (connected with triangles) in Fig. 2(a). Remarkably, it is found that the final fidelity with CD driving is even lower than that without CD driving. In other words, the CD driving, which is designed in a close-system set up, may unfortunately favor environment-induced effects.

The results shown in Fig. 2(b) are for very short LZ processes, with  $t_f = 0.1$  or  $v = 120$ . In this case, the driving time scale  $1/\sqrt{v} \ll \tau_B$ . Intuitively then, the environment has virtually no time to take effect. Indeed, for all the three cases shown in Fig. 2(b), the fidelity always stays extremely close to unity, even for  $\gamma = 5$  that represents a case with very strong system-environment coupling. By contrast, the bare  $H_{\text{LZ}}$  Hamiltonian without CD driving only yields fairly low fidelity values [see the black solid line in Fig. 1(c)]. An obvious conclusion is that the CD driving can work well only for fast sweeping cases. However, one should note that to realize very fast sweeping poses a challenge in actual implementations.

Fig. 3 depicts the final fidelity values as a function of the system-environment coupling strength  $\gamma$ , with or without CD driving. We choose two intermediate values of the sweeping rate to make an interesting comparison, with  $t_f = 2$  in panel (a) and  $t_f = 10$  in panel (b). In both panels, a crossing of the two fidelity curves occurs, which again demonstrates the existence of a regime that the CD driving leads to a lower fidelity than that without CD. Further calculations (not shown) suggest that for the present choice of all other parameters, this cross-

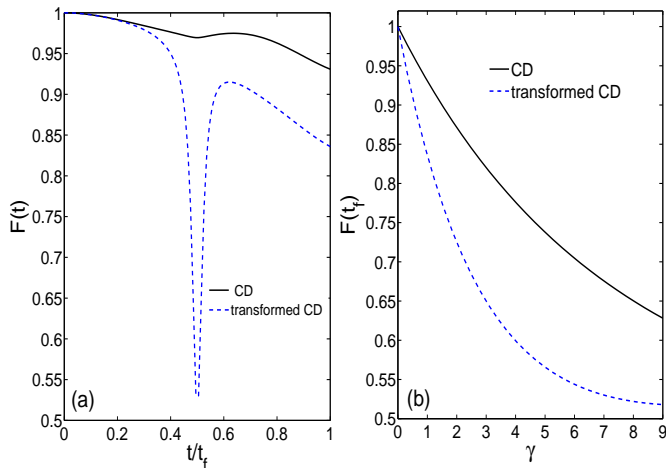


Figure 4: (Color online) (a) The fidelity with instantaneous adiabatic states versus scaled time  $t/t_f$ , with the system-bath coupling strength parameter  $\gamma = 1.0$ , for CD driving and transformed CD driving. The duration of the LZ processes is chosen to be  $t_f = 1$ . (b) Final fidelity values for CD driving and transformed CD driving, as a function of  $\gamma$ , with  $t_f = 1$ . Other system and environment parameters are the same as in Fig. 1.

ing occurs for  $0.7 < t_f < 40$ . Beyond this intermediate regime, i.e., for very fast sweeping, CD driving is always beneficial (see Fig. 2b), whereas for very slow sweeping, switching on CD driving does not cause a difference to the final fidelity values.

### B. A variant of counter-diabatic driving

In this subsection we study the performance of a variant of CD driving [47]. The idea behind transformed CD driving is as follows. If the main concern is to reach a final adiabatic state with high fidelity from a given initial adiabatic state, then there is no need to impose conditions on the evolution operator at intermediate times. Rather, only the unitary evolution operator associated with the whole quantum process is under consideration for designing a control field. One motivation to design such CD variants is to avoid the potential difficulties in the actual experimental realizations. Indeed, by considering different types of transformations from the adiabatic path of the instantaneous eigenstates of  $H_{LZ}$  to other paths in the Hilbert space, one obtains different driving fields to execute possible variants of CD, which we call transformed CD in this work.

In the present LZ problem, one transformed CD driving was introduced by del Campo [52]. It requires  $Z(t) = z_0 + 6\delta s^5 - 15\delta s^4 + 10\delta s^3$ , with  $s = t/t_f$  and  $\delta = z_f - z_0$ , with the transformed CD driving Hamiltonian given by

$$H_{\text{TCD}}(t) = [Z(t) - \dot{\eta}(t)] \frac{\sigma_z}{2} + P(t) \frac{\sigma_x}{2}, \quad (20)$$

where  $P = \sqrt{X^2 + \dot{\theta}_t^2}$ ,  $\theta_t = \text{arccot}[Z(t)/X]$  and  $\eta(t) = \arctan(\dot{\theta}_t/X)$ . As seen above, the main interesting feature of this transformed CD driving is that it does not contain  $\sigma_y$  and hence it is more analogous to the original  $H_{LZ}$  Hamiltonian.

It is now of great interest to compare the performance of the transformed CD driving with that of the above-studied CD driving, in the presence of an environment. Panel (a) of Fig. 4 shows the fidelity with instantaneous adiabatic states versus scaled time, with  $\gamma = 1$ . Somewhat expected, before the LZ process is over the fidelity of transformed CD is systematically smaller. Interestingly, this difference sustains at the end of the LZ process. That is, the final fidelity of the transformed CD is not as satisfactory as that of CD. Panel (b) Fig. 4 compares the final fidelity values as a function of  $\gamma$ . Clearly, for the whole shown range of system-bath coupling strength, transformed CD is less effective than CD in reaching the final target state (though in the unitary limit these two driving strategies give the same final result by construction). However, it remains an open question to see if it is possible for a transformed CD driving to be more robust against an environment than a default CD driving.

## V. CD DRIVING WITH CONTINUOUS DYNAMICAL DECOUPLING

Our results in previous sections clearly show that, so long as the quantum adiabatic operation is not very short, the presence of an environment poses a hurdle to realizing perfect adiabatic operations even with CD driving. We are thus motivated to consider a simple dynamical decoupling (DD) protocol to suppress the effect of system-bath coupling. This is highly nontrivial because in general, the introduction of a DD field can easily interfere with the design of CD driving. This section hence serves as a starting point to motivate further studies on this interesting problem.

For completeness, we first briefly introduce continuous DD, which is based on a continuous control Hamiltonian, denoted as  $H_{\text{DD}}$ , to effectively reduce system-bath coupling [61–64]. The total system-bath Hamiltonian is hence given by

$$\begin{aligned} H_{\text{tot}} &= H_S + H_{\text{DD}} + H_B + H_{\text{SB}}, \\ &\equiv H' + H_{\text{DD}}. \end{aligned} \quad (21)$$

A unitary transformation  $U_{\text{DD}}$  generated by  $H_{\text{DD}}$  alone can be expressed as

$$U_{\text{DD}}(t) = \hat{T} \exp \left[ -i \int_0^t H_{\text{DD}}(\tau) d\tau \right]. \quad (22)$$

In continuous DD,  $U_{\text{DD}}(t)$  satisfies two conditions. First,  $U_{\text{DD}}(t)$  should be periodic in time with a period denoted by  $t_D$ , i.e.,

$$U_{\text{DD}}(t + t_D) = U_{\text{DD}}(t). \quad (23)$$

Second,

$$\int_0^{t_D} U_{\text{DD}}^\dagger(\tau) H_{\text{SB}} U_{\text{DD}}(\tau) d\tau = 0. \quad (24)$$

The mechanism of continuous DD can then be easily understood. In particular, one may use  $H_{\text{DD}}$  as a reference Hamiltonian to define an interaction representation or a rotating frame. In that representation, the total Hamiltonian becomes  $\tilde{H}' = U_{\text{DD}}^\dagger H' U_{\text{DD}}$ . The associated total system-bath propagator becomes

$$\tilde{U}_{\text{tot}}(t) = \hat{T} \exp \left[ -i \int_0^t \tilde{H}'(\tau) d\tau \right]. \quad (25)$$

Dividing the total time interval ( $0 \sim t$ ) into  $N$  pieces of width  $t_D = t/N$  ( $N$  is a positive integer number) and using the Magnus expansion to the first order of  $1/N$  [65], one has

$$\begin{aligned} \tilde{U}_{\text{tot}}(t) &= \prod_{n=1}^N \hat{T} \exp \left[ -i \int_{(n-1)t_D}^{nt_D} \tilde{H}'(\tau) d\tau \right] \\ &\approx \prod_{n=1}^N \exp \left[ -i \int_{(n-1)t_D}^{nt_D} \tilde{H}'(\tau) d\tau \right]. \end{aligned} \quad (26)$$

Due to the conditions in Eqs.(23) and (24), terms with  $H_{\text{SB}}$  will vanish. That is,  $-i \int_{(n-1)t_D}^{nt_D} \tilde{H}'(\tau) d\tau \rightarrow -i \int_{(n-1)t_D}^{nt_D} [H_{\text{S}}(\tau) + H_{\text{B}}(\tau)] d\tau$ . Then  $\tilde{U}_{\text{tot}}(t)$  will factor into a product of independent evolution operators for the system and for the bath. Note also that at  $t = nt_D$ ,  $U_{\text{DD}} = 1$  and hence  $\tilde{U}_{\text{tot}}$  is precisely the overall system-bath evolution operator in the original representation. That is, in the limit of  $t_D \rightarrow 0$ , the system's evolution will completely decouple from that of the bath, with the evolution operator at  $t = nt_D$  given by  $\tilde{U}_{\text{S}}(t) = \hat{T} \exp \left[ -i \int_0^t U_{\text{DD}}^\dagger(\tau) H_{\text{S}}(\tau) U_{\text{DD}}(\tau) d\tau \right]$

The DD mechanism explained above makes it clear that under a DD field, the effective system Hamiltonian becomes that of  $\tilde{H}_{\text{S}}(t) = U_{\text{DD}}^\dagger(t) H_{\text{S}}(t) U_{\text{DD}}(t)$ . Before switching on a DD field,  $H_{\text{S}}(t)$  is meant to implement a CD driving. But now with DD, can the effective Hamiltonian  $\tilde{H}_{\text{S}}(t)$  still serve the purpose of CD driving or its variant? This can be a complicated question. Indeed, in general,  $U_{\text{DD}}$  might introduce transitions between different adiabatic states. However, this still does not exclude special solutions, one of which is discussed below.

Because the system-bath coupling is of the  $\sigma_x$  form, a suitable and simple choice of  $H_{\text{DD}}$  is [61, 62, 64]

$$H_{\text{DD}} = Y_D \sigma_y = \frac{\pi}{t_D} \sigma_y, \quad (27)$$

This DD Hamiltonian tends to rapidly rotate the  $\sigma_x$  coupling and then average the system-bath coupling to zero. On the other hand, in Sec. IV A it is noted that  $H_{\text{CD}} = \frac{\dot{\theta}}{2} \sigma_y$  [see Eq. (19)] alone suffices to realize an

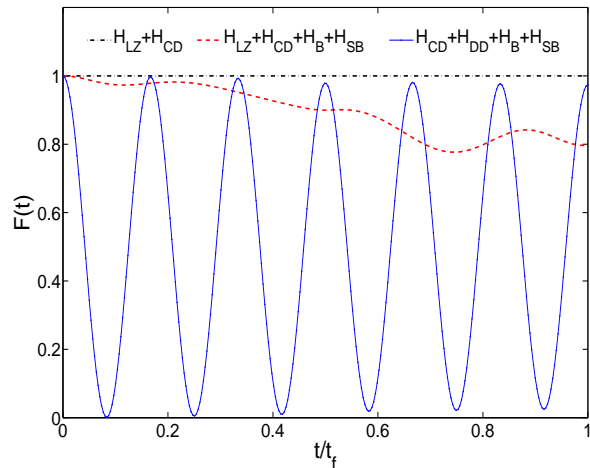


Figure 5: (Color online) The fidelity with instantaneous adiabatic states versus scaled time  $t/t_f$ , with  $t_f = 5$  and  $\gamma = 1$ . Other system and environment parameters are the same as in previous figures. (black) Dashed-dotted line represents a reference case, namely, CD driving without an environment, with  $H_{\text{S}} = H_{\text{LZ}} + H_{\text{CD}}$ . (red) Dashed line is for CD driving without DD, with the total Hamiltonian given by  $H_{\text{LZ}} + H_{\text{CD}} + H_{\text{SB}} + H_{\text{B}}$ . (blue) Solid line is for a case with “CD+DD” fields, with the total Hamiltonian given by  $H_{\text{CD}} + H_{\text{DD}} + H_{\text{SB}} + H_{\text{B}}$ .

adiabatic path precisely tracing the instantaneous adiabatic states of  $H_{\text{LZ}}$ . That is, the Hamiltonian  $H_{\text{LZ}}$  itself, which only introduces a dynamical phase to the instantaneous adiabatic states, is not essential, and can hence be excluded, from the perspective of CD driving. Remarkably then, if  $H_{\text{S}}$  is simply chosen as  $H_{\text{CD}}$ , then both  $H_{\text{DD}}$  and  $H_{\text{S}}$  are of the  $\sigma_y$  form, and so  $\tilde{H}_{\text{S}}(t) = U_{\text{DD}}^\dagger(t) H_{\text{S}}(t) U_{\text{DD}}(t) = H_{\text{S}}(t)$ . Therefore, at least in this special case of CD driving, a DD field is able to effectively decouple the system-bath coupling and at the same time retain the CD driving.

In Fig. 5, we present our computational results for a pure CD driving as well as a CD driving plus the above-introduced DD field, in terms of the fidelity with instantaneous eigenstates of  $H_{\text{LZ}}$ . As a reference point, The (black) dashed-dotted line depicts the case without environment, whose fidelity stays at unity. We then switch on the system-bath coupling with  $\gamma = 1$ . The (blue) solid line depicts the case with CD and DD, the oscillations in the fidelity are induced by  $H_{\text{DD}}$  and high fidelity values are reached periodically. The final fidelity  $F(t_f) \approx 0.97$  is much higher than if only CD driving is used (which gives  $F(t_f) \approx 0.8$  shown in the red dashed line). We have also checked that if we let  $H_{\text{S}} = H_{\text{LZ}} + H_{\text{CD}}$  to realize an adiabatic operation in the presence of an environment, then turning on a DD field as described above will not help to improve the fidelity.

Theoretically,  $t_D = \frac{\pi}{Y_D}$  describes the rotation period



of  $U_{\text{DD}}$ . In accord with the above theory of continuous DD, only if  $Q \equiv \frac{t_f}{t_D}$  is an integer, then one might achieve the best final fidelity. In the actual implementation, e.g., the (blue) solid line in Fig. 5, the peak-value of the final fidelity occurs for  $Q \simeq 5.94$  instead of  $Q = 6$ . This small deviation can be traced back to the approximations made in the first-order Magnus expansion. Note also that the associated DD field amplitude is 3.7 in dimensionless units, whereas the peak amplitude of the CD driving field is about 2.4. By contrast, if we boost the final fidelity to  $F(t_f) \approx 0.97$  by solely increasing the sweeping rate in the CD driving without using DD, the peak strength of the CD field will be as large as 15. That is to say, the use of a DD field is indeed helpful to battle against an environment in the realization of CD driving.

## VI. CONCLUDING REMARKS

In this work we have investigated finite-time Landau-Zener processes in the presence of an environment, which is modeled by a broadened cavity mode at zero temperature. Such an environment model allows us to use the hierarchy equation method to obtain numerically exact results of the dynamics without any approximations.

The fidelity for the system to be found at the final target adiabatic state shows a non-monotonic dependence on the system-bath coupling strength and on the sweeping rate in the energy bias parameter. This signals an interesting competition between the otherwise unitary LZ process and environment-induced relaxation and excitation. More importantly, it is found that an environment

can affect the performance of CD driving significantly. If the LZ process is not short enough, the addition of CD driving may lend more opportunities to the environment to degrade the performance even further. It is also found that different versions of CD driving can have different degrees of robustness against environment effects.

Our results indicate that more studies of CD driving in the presence of an environment will be fruitful. As a starting point, we discussed the possibility of combining CD driving with dynamical decoupling (DD). At least for the simple case we investigated, it is possible to combine CD and DD to realize high-fidelity adiabatic manipulation in the presence of an environment, without requiring the process to be extremely fast.

## Acknowledgements

Z.S. is supported by the National Natural Science Foundation of China under Grants No. 11375003, the Program for HNUEYT under Grant No. 2011-01-011, the Zhejiang Natural Science Foundation with Grant No. LZ13A040002, the funds for the Hangzhou-City Quantum Information and Quantum Optics Innovation Research Team. D.P. acknowledges support by the SUTD Start-Up Grant EPD2012-045. D.P. and J.G. are also supported by Singapore MOE Academic Research Fund Tier-2 project (Project No. MOE2014-T2-2-119, with WBS No. R-144-000-350-112). J.G. also wishes to thank Y. Tanimura for teaching his hierarchy equation method at NUS.

- 
- [1] S. Shevchenko, S. Ashhab, F. Nori, Phys. Rep. **492**, 1 (2010).
  - [2] S. Gasparinetti, P. Solinas, J. P. Pekola, Phys. Rev. Lett. **107**, 207002 (2011).
  - [3] C. Kasztelan, *et al.*, Phys. Rev. Lett. **106**, 155302 (2011).
  - [4] J.-N. Zhang, C. P. Sun, S. Yi, F. Nori, Phys. Rev. A **83**, 033614 (2011).
  - [5] A. Altland, V. Gurarie, Phys. Rev. Lett. **100**, 063602 (2008).
  - [6] Y.-A. Chen, S. D. Huber, S. Trotzky, I. Bloch, E. Altman, Nature Phys. **7**, 61 (2011).
  - [7] M. G. Bason, *et al.*, Nature Phys. **8** 147 (2012).
  - [8] D. M. Berns, *et al.*, Nature **455**, 51 (2008).
  - [9] A. Zenesini *et al.*, Phys. Rev. Lett. **103**, 090403 (2009).
  - [10] J.Q. You, F. Nori, Physics Today **58** (11), 42 (2005).
  - [11] J.Q. You, F. Nori, Nature **474**, 589 (2011).
  - [12] M. Sillanpää, *et al.*, Phys. Rev. Lett. **96**, 187002 (2006).
  - [13] G. Z. Sun, *et al.*, Nature Communications **1** 51 (2010).
  - [14] M. Wubs, *et al.*, New J. Phys. **7**, 218 (2005).
  - [15] J. Keeling, V. Gurarie, Phys. Rev. Lett. **101**, 033001 (2008).
  - [16] Z. Sun, J. Ma, X. Wang, F. Nori, Phys. Rev. A **86**, 012107 (2012).
  - [17] M. Wubs, K. Saito, S. Kohler, P. Hänggi, Y. Kayanuma, Phys. Rev. Lett. **97**, 200404 (2006).
  - [18] K. Saito, M. Wubs, S. Kohler, Y. Kayanuma, P. Hänggi, Phys. Rev. B **75**, 214308 (2007).
  - [19] J. E. Avron, M. Fraas, G. M. Graf, P. Grech, Commun. Math. Phys. **305**, 633–639 (2011).
  - [20] L. Zhou, D. Y. Tan, J. Gong, arXiv:1507.07331
  - [21] P. Nalbach, M. Thorwart, Phys. Rev. Lett. **103**, 220401 (2009).
  - [22] P. P. Orth, A. Imambekov, K. Le Hur, Phys. Rev. A **82**, 032118 (2010).
  - [23] R. S. Whitney, M. Clusel, T. Ziman, Phys. Rev. Lett. **107**, 210402 (2011).
  - [24] C. Xu, A. Poudel, M. G. Vavilov, Phys. Rev. A **89**, 052102 (2014).
  - [25] V. L. Pokrovsky, D. Sun, Phys. Rev. B **76**, 024310 (2007).
  - [26] S. Javanbakht, P. Nalbach, M. Thorwart, Phys. Rev. A **91**, 052103 (2015).
  - [27] A. Dodin, S. Garmon, L. Simine, D. Segal, J. Chem. Phys. **140**, 124709 (2014).
  - [28] P. P. Orth, A. Imambekov, K. Le Hur, Phys. Rev. B **87**, 014305 (2013).
  - [29] Y. Tanimura, P. G. Wolynes, Phys. Rev. A **43**, 4131 (1991).
  - [30] M. Tanaka, Y. Tanimura, J. Chem. Phys. **132** 214502

- (2010).
- [31] A. G. Dijkstra, Y. Tanimura, Phys. Rev. Lett. **104**, 250401 (2010).
- [32] A. Ishizaki, Y. Tanimura, J. Phys. Chem. A **111**, 9269 (2007).
- [33] Y. Tanimura, J. Phys. Soc. Jpn. **75**, 082001 (2006).
- [34] J. S. Jin, X. Zheng, Y. J. Yan, J. Chem. Phys. **122**, 041103 (2004).
- [35] J. Xu, R.-X. Xu, Y. J. Yan, New J. Phys. **11**, 105037 (2009).
- [36] M. Sarovar, A. Ishizaki, G. R. Fleming, K. B. Whaley, Nature Phys. **6**, 462 (2010);
- [37] J. Ma, Z. Sun, X. Wang, F. Nori, Phys. Rev. A **85**, 062323 (2012).
- [38] W. Guo, J. Ma, X. Yin, W. Zhong, X. Wang, Phys. Rev. A **90**, 062133 (2014).
- [39] E. Torrontegui, *et al.*, Adv. At. Mol. Opt. Phys., **62** 117 (2013).
- [40] M. Demirplak, S. A. Rice, J. Phys. Chem. A **107**, 9937 (2003);
- [41] M. Demirplak, S. A. Rice, J. Phys. Chem. B **109**, 6838 (2005);
- [42] M. Demirplak, S. A. Rice, J. Chem. Phys. **129**, 154111 (2008).
- [43] M. V. Berry, J. Phys. A: Math. Theory **42**, 365303 (2009).
- [44] S. Guérin, V. Hakobyan, H. R. Jauslin, Phys. Rev. A **84**, 013423 (2011).
- [45] S. Masuda, K. Nakamura, Phys. Rev. A **84**, 043434 (2011).
- [46] X. Chen, I. Lizuain, A. Ruschhaupt, D. Guéry-Odelin, J. G. Muga, Phys. Rev. Lett. **105**, 123003 (2010).
- [47] S. Ibáñez, X. Chen, E. Torrontegui, J.G. Muga, A. Ruschhaupt, Phys. Rev. Lett. **109**, 100403 (2012).
- [48] X. Chen, J. G. Muga, Phys. Rev. A **82**, 053403 (2010).
- [49] R. Bowler, *et al.*, Phys. Rev. Lett. **109**, 080502 (2012).
- [50] M. S. Sarandy, E. I. Duzzioni, R. M. Serra, Phys. Lett. A **375**, 3343 (2011).
- [51] H.-K. Lau, D. F. V. James, Phys. Rev. A **85**, 062329 (2012).
- [52] A. del Campo, Phys. Rev. Lett. **111**, 100502 (2013).
- [53] Y. Li, L. A. Wu, Z. D. Wang, Phys. Rev. A **83**, 043804 (2011).
- [54] A. del Campo, J. Goold, M. Paternostro, Sci. Rep. **4**, 6208 (2014).
- [55] Y. Zheng S. Campbell, G. De Chiara, D. Poletti, arxiv:1509.01882 (2015).
- [56] G. Vacanti, R. Fazio, S. Montangero, G. M. Palma, M. Paternostro, V. Vedral, New J. Phys. **16**, 053017 (2014).
- [57] Y. H. Issoufa, A. Messikh, Phys. Rev. A **90**, 055402 (2014).
- [58] L. Viola, S. Lloyd, Phys. Rev. A **58**, 2733 (1998).
- [59] L. Viola, E. Knill, S. Lloyd, Phys. Rev. Lett. **82**, 2417 (1999).
- [60] S. Maniscalco, *et al.*, Phys. Rev. Lett. **100**, 090503 (2008).
- [61] F. F. Fanchini, J. E. M. Hornos, and R. d. J. Napolitano, Phys. Rev. A **75**, 022329 (2007).
- [62] F. F. Fanchini, J. E. M. Hornos, and R. d. J. Napolitano, Phys. Rev. A **76**, 032319 (2007).
- [63] X. Xu, *et al.*, Phys. Rev. Lett. **109**, 070502 (2012).
- [64] A. Z. Chaudhry and J. Gong, Phys. Rev. A **85**, 012315 (2012).
- [65] W. Magnus, Commun. Pure Appl. Math. **7**, 649 (1954).